Tribology International 88 (2015) 317–326

Contents lists available at ScienceDirect

Tribology International

journal homepage: www.elsevier.com/locate/triboint

Gearbox power loss. Part III: Application to a parallel axis and a planetary gearbox

Carlos M.C.G. Fernandes [a,*], Pedro M.T. Marques [a], Ramiro C. Martins [a], Jorge H.O. Seabra [b]

[a] INEGI, Universidade do Porto, Campus FEUP, Rua Dr. Roberto Frias 400, 4200-465 Porto, Portugal
[b] FEUP, Universidade do Porto, Rua Dr. Roberto Frias s/n, 4200-465 Porto, Portugal

ARTICLE INFO

Article history:
Received 6 January 2015
Received in revised form
27 February 2015
Accepted 20 March 2015
Available online 27 March 2015

Keywords:
Gearboxes
Power loss
Wind turbine gear oils

ABSTRACT

In the third part of this work, the rolling bearing torque loss model, the lubricant factor extracted from the FZG tests with wind turbine gear oils and the loss factor for helical gears, developed in Part I and Part II of this work, will be applied to predict the power loss in a parallel axis and a planetary gearbox. The numerical results obtained are compared with those from experimental tests.

1. Introduction

In the first part, thrust roller and ball bearings were tested for power loss in a modified four ball machine using different ISO VG 320 wind turbine gear oils (a mineral (MINR), a poly-alpha-olephin (PAOR), a mineral with PAMA viscosity modifier (MINE) and a poly-alkyleneglycol (PAGD)). The coefficient of friction in the rolling bearings was determined, allowing a better correlation between the numerical and measured torque loss. The model for the friction power loss in the gear meshing was also calibrated. In the second part of this work the lubricant factor (X_L) that is used to adapt the classic gear mesh coefficient of friction formula originally proposed by Schlenk et al. [1] was obtained for four different wind turbine gear oils after some experiments with helical and spur gears in an FZG test rig.

The aim of this third part is to apply the models developed in part I [2] and part II [3] of this work in order to predict, as accurately as possible, the gearbox power loss.

2. Gearbox test rig

The gearbox test rig (Fig. 1) follows the principle of recirculating power. This test rig allows the testing of gearboxes of different size and type, given that they fit within the dimensional constraints and allow for reducer/multiplier operation. Two gearboxes are used, one as speed multiplier and the other as speed reducer, in order to close the circulating power loop. This test rig allows input speeds from 100 to 1900 rpm and input torques from 100 to 1300 N m. The gearbox oil sump temperature is set free.

The gearbox test rig allows monitoring and recording several operating parameters, namely input and output torque/speed of the test gearbox; room temperature; oil sump temperature in the test gearbox in two locations; external wall temperature of the housing on both test and slave gearboxes in various points.

Industrial grade 3 wire *Pt*100 RTD's and Type K thermocouples were used to monitor the temperatures in these points.

3. Parallel axis gearbox

In previous works [4] the authors have studied the power loss behaviour of a parallel axis gearbox. This time, the numerical results are re-evaluated taking into account the coefficient of friction derived from the FZG tests and the modifications to the rolling bearings power loss model, reported in parts I and II of this work.

Fig. 2 shows a schematic view of the test gearbox. This gearbox has three shafts where five gears are mounted. The gears in the middle shaft are keyed while the gears on the first and third shafts are mounted over needle bearings. All shafts are supported by ball or roller bearings. The test gearbox allows the selection of two different kinematic relations. All tests were conducted with the test gearbox working as speed multiplier ($u \approx 2.3$).

Abbreviations: TRB, tapper roller bearing; DGBB, deep groove ball bearing; NRB, needle roller bearing; N.A., not available; N.O., not operating; N.E., non-existent

* Corresponding author.
E-mail address: cfernandes@inegi.up.pt (C.M.C.G. Fernandes).

http://dx.doi.org/10.1016/j.triboint.2015.03.029
0301-679X/

Notation and Units

a	axis distance (mm)
b	tooth face width (mm)
d_{sh}	shaft seal diameter (mm)
F_{bt}	tangential force on the base plane (N)
m	module (mm)
M_t	bearing friction torque (N mm)
M'_{rr}	rolling friction torque (N mm)
M_{sl}	sliding friction torque (N mm)
M_{drag}	friction torque of drag losses (N mm)
M_{seal}	friction torque of seals (N mm)
n_p	number of planets (–)
P_{IN}	mesh input power (W)
P^g_{IN}	gearbox input power (W)
P_V	model total power loss (W)
P_{VL}	rolling bearings power loss (W)
P_{VZ0}	no-load gears power loss (W)
P_{VZP}	meshing gears power loss (W)
P_{VD}	seals power loss (W)
Q	heat lost by dissipation (W)
R_a	arithmetic average roughness of pinion and gear (μm)
T_{oil}	oil sump temperature (°C)
T_{room}	room temperature (°C)
u	gear ratio (z_2/z_1) (–)
v_t	pitch line velocity (m/s)
x	addendum modification (–)
XL	lubricant parameter (–)
z	number of teeth (–)
α	pressure angle (deg)
$\alpha \cdot A$	Global heat transfer coefficient (W/K)
β	helix angle (deg)
ν_{oil}	oil kinematic viscosity at operating oil sump temperature (mm^2/s)
$\Delta T_{or} =$	$T_{oil} - T_{room}$ deg
$\Delta T_{ow} =$	$T_{oil} - T_{wall}$ deg
ϕ_{bl}	sliding friction torque weighting factor (–)
ϕ_{ish}	inlet shear heating reduction factor (–)
ϕ_{rs}	kinematic replenishment/starvation reduction factor (–)
μ_{bl}	coefficient of friction in boundary film lubrication (–)
μ_{EHD}	coefficient of friction in full film lubrication (–)
μ_{sl}	sliding coefficient of friction (–)

The transfer gearbox is filled with 2 l of a wind turbine gear oil with the physical and chemical properties described in the first part of the work [2].

Table 1 displays the main geometric properties of the gears used in the test gearbox. Table 2 shows information about the rolling bearings installed in the test gearbox.

Table 3 shows the test sequence and imposed input speed and torques.

3.1. Experimental results

Fig. 3 shows the experimental results in terms of stabilized operating temperatures. These results clearly indicate that usually PAGD promotes the lowest power loss and MINR the highest. The test with MINR at the highest load and speed was disregarded due to expected operating temperatures well above 100 °C. PAOR and MINE performed identically, and are positioned between MINR and PAGD.

3.2. Power loss modelling

The load dependant power loss model that was used to predict the power loss generated in the parallel axis gearbox is the same that was employed to derive the gears coefficient of friction for the torque loss measurements in Part II of the current work [3]. The model will be applied considering the power loss generated in the gearbox for the tested operating conditions for rolling bearings (Appendix A), gears (Appendix B) and seals (Appendix C).

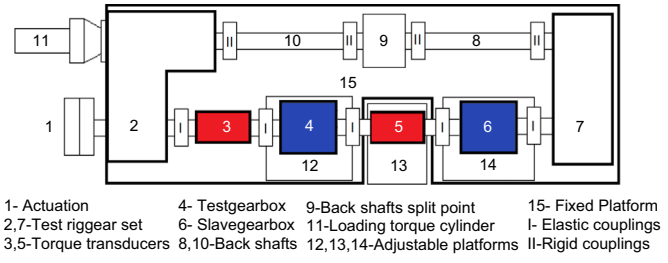

Fig. 1. Top view scheme of the gearbox test rig.

3.2.1. Gears churning loss model

For splash-lubricated gears, oil churning is a major source of power loss which is related to the fluid circulation generated by rotating gears partly immersed in a lubricant [5].

Recently, Changenet et al. [5] presented a gear churning loss model based on a dimensional analysis approach and a series of experimental tests to tune the model. This model was selected because it seeks to overcome some of the limitations of previous models [6–9] which were also based on empirical studies.

The gear churning loss model proposed by Changenet et al. [5] depends on a Reynolds number that describes the laminar–turbulent transition which was also determined after the experimental results.

The laminar–turbulent flow transition inside an oil sump lubricated gearbox is difficult to determine mainly due to the almost infinite combination of design features that exists. In previous works the authors applied this gear churning loss model to the parallel axis gearbox [10] and verified that one of the main reasons for the discrepancy between the numerical and experimental results was on the prediction of the gear churning loss. Using the Reynolds number calculated for single pinions did not allow a correct simulation of the churning losses, underestimating the churning losses importance. Based on the stabilized operating temperatures, the authors [10] found a way to determine an approximate laminar–turbulent transition point that was used to adjust the gear churning loss model.

3.3. Modelling results

Fig. 4 show the calculated power loss as well as each one of its components. For the tested operating conditions the meshing losses dominate the power loss. Depending on the oil nature, namely dynamic viscosity, the gear churning losses seem to be higher than the bearings power loss.

The measured values of power loss are presented with the power loss model predictions in Fig. 5.

At stabilized conditions the heat that is lost to the environment through the gearbox is equal to the power loss. Eq. (1) shows the relation between the stabilized operating temperature and the power that is dissipated through the gearbox:

$$Q = \alpha \cdot A \cdot \Delta T \tag{1}$$